Magazine of Concrete Research
Volume 67 Issue 2

Anchorage behaviour and development length of headed bars in exterior beam–column joints
Dhake, Patil and Patil

Magazine of Concrete Research, 2015, **67**(2), 53–62
http://dx.doi.org/10.1680/macr.14.00144
Paper 1400144
Received 14/05/2014; revised 27/06/2014; accepted 30/06/2014
Published online ahead of print 19/08/2014

ice
Institution of Civil Engineers
publishing

Anchorage behaviour and development length of headed bars in exterior beam–column joints

Pravinchandra D. Dhake
Research Scholar, Applied Mechanics Department, SVNIT-Surat, Gujrat, India

Yogesh D. Patil
Assistant Professor, Applied Mechanics Department, SVNIT-Surat, Gujrat, India

Hemant S. Patil
Professor, Applied Mechanics Department, SVNIT-Surat, Gujrat, India

Six exterior beam–column joint specimens with and without transverse shear reinforcement were constructed and tested under cyclic loading to assess the anchorage strength of headed bars with short development length. The test results demonstrated that the beam–column specimen without transverse shear reinforcement can exhibit satisfactory seismic behaviour with headed bars up to a drift ratio of 3%; above this the role of transverse shear reinforcement is vital. The test results also indicated that hysteretic behaviour of exterior beam–column joints with headed bars was superior to joints constructed and tested with 90° bent bars with sufficient anchorage length.

Notation

A_b	bar area (mm^2)
A_{brg}	net bearing area (mm^2)
A_{head}	gross head area (mm^2)
A_{obs}	area of obstruction (mm^2)
d_b	bar diameter (mm)
f'_c	specified concrete cylinder strength (MPa)
f_y	specified strength of headed bar (MPa)
l_{dt}	development length in tension (mm)
M_n	nominal flexural strength (kNm)
P_{max}	ultimate load (kN)
P_n	nominal flexural load (kN)
Δ_{max}	ultimate displacement (mm)
Δ_y	yield displacement (mm)
Δ_{max}/Δ_y	displacement ductility
μ	displacement ductility
ψ_e	factor based on reinforcement coating

Introduction

Reinforced concrete can act successfully as a composite material only when the constituent materials, concrete and reinforcement deform and carry force together. Normally in a reinforced concrete structure, the load is not applied directly to the reinforcement, but acts on the concrete (Park and Paulay, 1974). The reinforcement can receive its share of load only when the load is transferred to it from the concrete. For effective transfer of load from one member to another there must be proper anchorage between members of composite material. In general, anchorage is achieved by a combination of bond (adhesion, friction and bearing against transverse ribs) and bearing on 90° and 180° hooks. Current code provisions (ACI 352R-02 (ACI–ASCE, 2002), IS 13920 (BIS, 1993) and IS 456 (BIS, 2000)) specify the development length of straight as well as hooked bars. Placement of these bars with large development lengths is the major problem at the exterior beam–column junctions. Use of high-strength steel makes this problem more critical. The bends and tails of the hooked bars create congestion, which hinders concrete placement and compaction inside the joint during casting; but concrete compressive strength is more important than the number of joint hoops to define shear capacity of the joint (Alva *et al.*, 2007). Some attempts by researchers have been made to minimise reinforcement congestion at the exterior beam–column joints. Use of steel plates for anchoring the longitudinal reinforcement of beams (Kotsovou and Mouzakis, 2011) minimised cracking and deformation of the joints. Use of steel fibre reinforcement concrete at the junction reduced the number of lateral ties without affecting ductility (Patel *et al.*, 2013).

Headed bars can offer a potential solution to these problems and may also ease reinforcement laying, concrete placement and compaction (Chun *et al.*, 2007). To study the parameters influencing the behaviour of mechanical anchorage, research was conducted on idealised evaluations where headed bars were pulled from concrete blocks (Wright and McCabe, 1997) and columns (Bashandy, 1996; Chun *et al.*, 2009). A compression–compression–tension (CCT) node test was conducted on beam specimens with headed bars; the variables being studied were angle of compression strut, head size and shape, bar diameter and confining effect (Thompson *et al.*, 2005). By using actual specimens of beam–column joints, the experimental work was conducted to

assess the effectiveness of headed bars with the emphasis on joint detailing (Chun *et al.*, 2007; Wallace *et al.*, 1998) and small head size (Kang *et al.*, 2010).

Development length and details of headed bars

Headed bars with different head shapes such as square, rectangular, circular and elliptical can be used, but top cast bar effect can be the major problem with square, rectangular and horizontally oriented elliptical shapes. A vertically oriented elliptical shape increases distance between the two layers of reinforcement. Hence bars with circular heads with $(A_{brg}/A_b) = 4$ were used in the present study.

The net bearing area A_{brg} is defined as the gross head area A_{head} minus the area of obstruction A_{obs}. The larger head size with ratio $(A_{brg}/A_b) = 9$ as recommended by ACI 352R-02, is often impracticable. Prior experimental research has shown that the ratio (A_{brg}/A_b) of approximately 4 is appropriate to ensure proper anchorage (Chun *et al.*, 2007; Thompson *et al.*, 2005) and the same is recommended by ACI 318-08 (ACI, 2008) as minimum head size.

As per ACI 352R-02, the development length in tension (l_{dt}) for headed bars for a type 2 joint is defined as

1. $$l_{dt} = \frac{0{\cdot}179 f_y d_b}{(f'_c)^{1/2}} \text{ for a type 1 joint}$$

2. $$l_{dt} = \frac{0{\cdot}15 f_y d_b}{(f'_c)^{1/2}} \text{ for a type 2 joint}$$

In Equation 2 the stress multiplier 1·25 is considered to account for over-strength and strain-hardening of reinforcement. This provision defines a type 1 connection as the connection which has members that are designed to satisfy strength requirements without significant inelastic deformation, and a type 2 connection as the connection that has members required to dissipate energy through reversals of deformation into the inelastic range. The length should be measured from the back face of the head plate to the beam interface for a type 1 connection, whereas for a type 2 connection it is measured up to the outer face of the joint hoop only.

ACI 318-08 also defines the development length in tension (l_{dt}) for headed bars as follows

3. $$l_{dt} = \frac{0{\cdot}19 \psi_e f_y d_b}{(f'_c)^{1/2}} \geqslant \text{the larger of } 8d_b \text{ and } 152 \text{ mm}$$

The length should be measured from the inner face of the head plate to the beam–column interface. Where f_y is the specified strength of headed bar in MPa; f'_c is the specified concrete cylinder strength in MPa; d_b is the bar diameter in mm; $\psi_e = 1{\cdot}2$ for epoxy-coated bars and 1·0 for other cases. For the measured material properties of the present experimental work the development length works out to be $17d_b$ as per Equation 1, $14{\cdot}2d_b$ as per Equation 2 and $18d_b$ as per Equation 3.

In many developing countries the practice of providing column width as 200 to 230 mm is very common, particularly in residential structures of up to five storeys. For the bars entering the column along the depth of the column, sufficient embedded length is available, but for bars entering along the width of the column, only a short development length is available. In the present research work the column depth was considered as 200 mm so that the available development length is $11d_b$ (Figure 1), which is measured from the inner face of the head plate to the outer face of the joint hoop.

Research significance

An experimental study was devised to assess the effect of critical influencing factors such as short development length, position of head plate and effect of transverse reinforcement in the joint. Here the meaning of short development length is as compared to previous research (Bashandy, 1996; Wright and McCabe, 1997) and code provisions (ACI 352R-02 (ACI–ASCE, 2002) and ACI 318-08 (ACI, 2008)).

Six one-third scale exterior beam–column joint specimens were constructed and tested in which one specimen had 90° hook bars and the remaining specimens had headed bars. A headed bar was formed by inserting the end portion of a straight reinforcing bar into a centrally drilled hole in a 10 mm thick circular plate and welding it from both sides. Use of headed bars makes it very simple to insert a beam reinforcement cage into the column reinforcement cage and substantially relieves reinforcing congestion. The various parameters such as crack pattern, hysteresis behaviour, ultimate load, modes of failure, energy dissipation, displacement ductility and stiffness degradation were studied.

Experimental investigations

Material properties and concrete mix design

The materials required for the experimental work were tested in the laboratory to obtain the necessary data for mix design. Pozzolana Portland cement (PPC) of 53 grade (conforming to IS 1489, part I (BIS, 1991)) and natural river sand with specific gravity 2·69 and fineness modulus 3·5, which conforms to grading zone II (IS 383 (BIS, 1970)), were used as fine aggregate. Crushed basalt with maximum size of 20 mm and specific gravity 2·79 was used as coarse aggregate. Concrete mix design was carried out for concrete grade M30 for medium workability. Thermo-mechanically treated ribbed bars of diameter 12 mm (here denoted in the figures as #12) were used as longitudinal reinforcement of beams and columns, whereas 6 mm diameter bars (denoted as #6 in the figures) were used as transverse

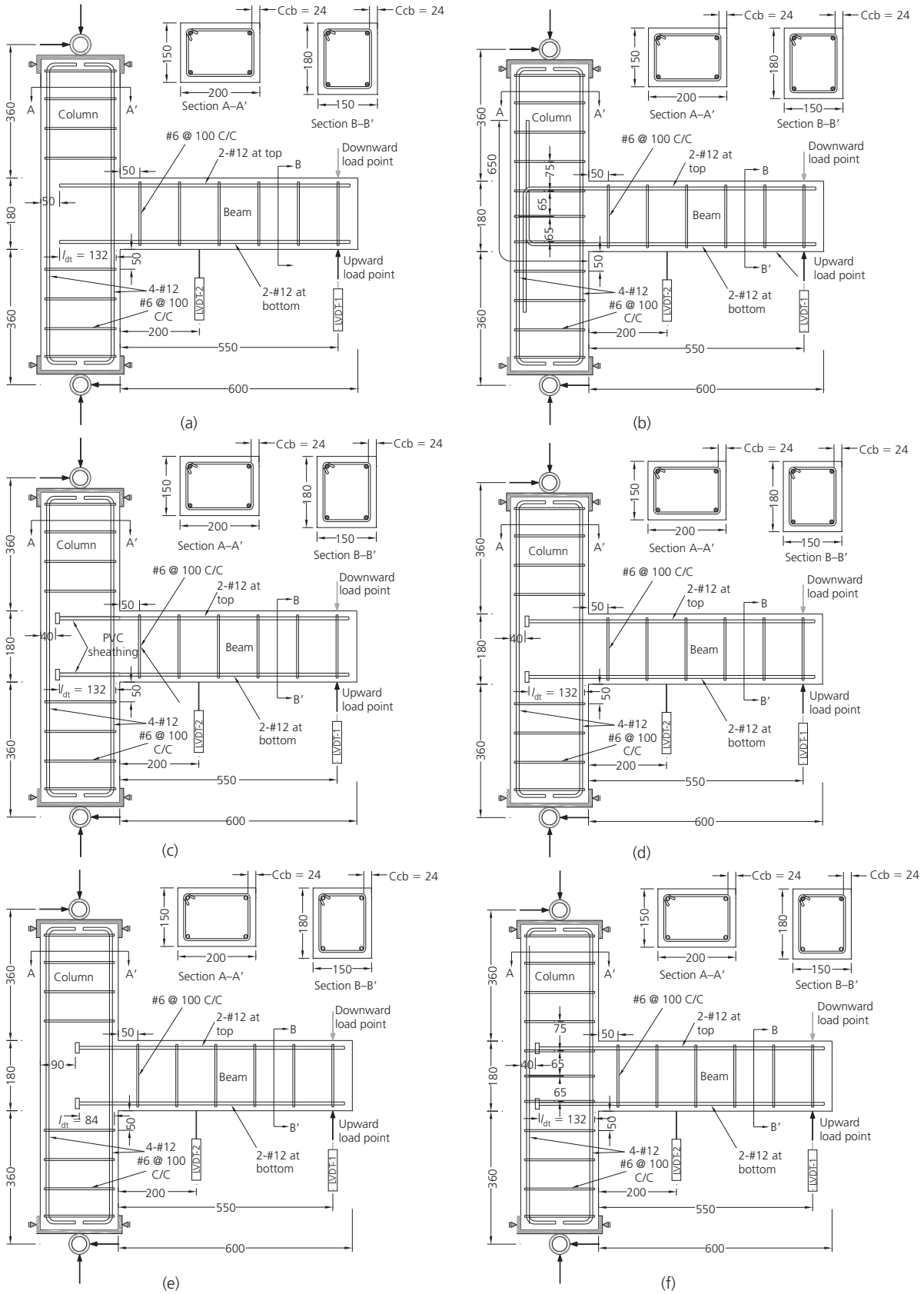

Figure 1. Reinforcement details of specimens: (a) J1; (b) J2; (c) J3; (d) J4; (e) J5; (f) J9

reinforcement. Three bars were tested for mechanical properties. The 0·2% proof stress of #12 bars was in the range 520–530 MPa, while the range for #6 bars was 500–515 MPa. Figure 2 shows the stress–strain curves of reinforcement steel.

Details of specimens

In all the test specimens the dimension of the beam was 150 × 180 mm with length of 600 mm and the column size was 150 × 200 mm with total height of 900 mm from top hinge support to bottom hinge support. The lengths of columns and beams were defined to simulate the nearest inflection points in the beam and column framing into the joint. In all the specimens the main reinforcement provided in the beam was two 12 mm diameter bars at the top and two 12 mm diameter bars at the bottom, whereas in the column four 12 mm diameter bars reinforcement was provided. In the beam 6 mm diameter at 100 mm centre-to-centre stirrups were provided, and in the columns 6 mm diameter at 100 mm centre-to-centre ties. The details of the specimens are shown in Figure 1.

The headed bars in specimens J3, J4 and J9 extended into the joint as far as possible, so that the head was located within the concrete compression strut. Specimen J1 was, along with the straight bars, embedded up to $11d_b$. Specimen J2 was, along with 90° hook bars, embedded up to $54d_b$ ($62d_b$–$8d_b$ for a 90° hook). The detailing of reinforcement of specimen J2 was as per IS 13920:1993 (BIS, 1993). Specimens J3 and J4 were with headed bars with development length $11d_b$, with the difference that in specimen J3 the embedded bar was coated with polyvinyl chloride (PVC) sheathing. To investigate the contribution of the concrete to the anchorage strength, transverse reinforcement was not placed in the joint in specimens J3 and J4. For specimen J5, the head was placed near the centre of the joint, where the head was outside the concrete compression strut ($l_{dt} = 7d_b$). Specimen J9 was detailed with transverse reinforcement and headed bars were extended for $l_{dt} = 11d_b$. In all specimens, cover to bar was 24 mm (Ccb = $2d_b$) and effective depths for beam and column were 150 mm and 170 mm respectively.

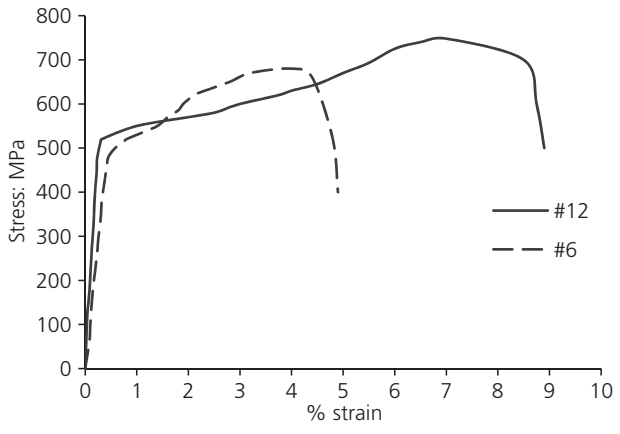

Figure 2. Stress–strain curve for reinforcement steel

The moulds were placed over a smooth surface and a reinforcement cage was arranged in each mould, ensuring specified cover to bars. The concrete was placed into the mould immediately after mixing and then well compacted. The moulds were removed 24 h after casting. All the specimens were cured in water for 28 d. After 28 d of curing the specimens were dried in air and whitewashed to improve crack visibility.

Test set-up and instrumentation

The specimens were tested in a reaction frame. The test set-up is shown in Figure 3. Each of the test specimens was subjected to cyclic load reversals to simulate earthquake loadings. A 1000 kN capacity calibrated hydraulic jack, mounted vertically on the frame, was used to apply axial load on the column. A constant load of 100 kN, which is about 20% of the axial capacity of the column, was applied to the columns to hold the specimens in position and to simulate column axial load. Another two 500 kN capacity hydraulic jacks were used to apply reverse cyclic loading. The load was applied at a distance of 50 mm from the free end of the beam face. The load was measured by inserting a load cell between the jack and the beam face. The test was displacement (drift ratio) controlled and the specimen was subjected to an increasing cyclic displacement, where the drift ratio (DR) is defined as the ratio of deflection Δ of the load point to the distance between the load point and the centreline of the column. Figure 4 shows the loading history in terms of applied cycles plotted against storey drift ratio. The deflections were measured by linear variable differential transducers (LVDTs) at the beam free end tip (at loading point), at a distance of 200 mm from the beam–column junction.

Strength prediction

Nominal flexural strength (M_n) was predicted for each specimen. The nominal flexural strength was defined as the moment at which beam yielding would occur, when the contribution of reinforcement in the compression zone and the measured material properties were used in the analysis. The partial safety factors for materials were not considered in either case. The test day compressive strengths of the control concrete cubes and cylinders were 35 MPa and 30 MPa respectively.

Test results and discussion

Modes of failure and cracking behaviour

Four modes of failure were established. Joint shear failure (JF) was characterised by gradual loss of load-carrying capacity before the formation of a plastic hinge in the adjacent beam. Beam flexure failure (BF) was identified by gradual loss of load-carrying capacity after the formation of a plastic hinge in the region of the beam adjacent to the joint. The combined mode of failure is denoted by BJF. Concrete breakout failure was characterised by diagonal cracks radiating from both sides of the head.

The crack pattern of all the specimens at the end of the test is

Figure 3. Test set-up

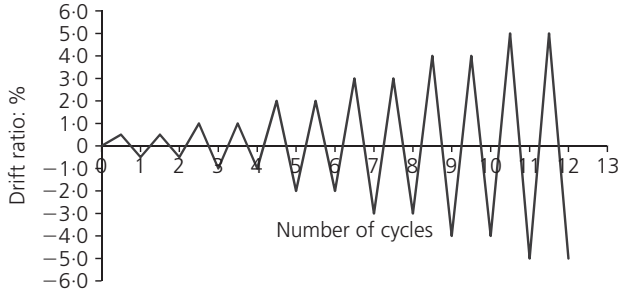

Figure 4. Cyclic loading history

shown in Figure 5. In specimen J1 the initial joint shear cracks appeared diagonally during DR 0·5%, followed by propagation of diagonal cracks up to DR 3%. It did not reach theoretical beam flexural capacity until the end of the test.

In specimen J2 initial cracks appeared at the beam interface during DR 0·5%, and these propagated and widened in the subsequent cycles. The diagonal cracks initiated at DR 1% and extended along the diagonal up to DR 4%. Many other cracks also appeared across the joint region.

The specimens J3 and J4 have the same reinforcement detailing except for the PVC sheathing provided to the bars in the joint region in specimen J3. Specimen J3 showed increased capacity at initial loading cycles (up to DR 3%), as compared to specimen J4. Additionally, the PVC sheathing decreased the degree of surface cracking at the joint region. A major crack occurred at the beam–column interface, the width of which increased in the subsequent loading cycles. Although some diagonal cracks occurred in the joint region, their width did not increase in the subsequent cycles. This occurred because the splitting tensile force and cracking associated with the bond of the ribbed bars were eliminated and, at yielding of the bars, the non-bonded embedded length increased with the load cycles. Specimens J2 and J3 incorporated damage in the joint region owing to shear cracking, as well as in the beam region near the interface.

In specimen J4 all the cracks appeared diagonally at the joint region. No cracks were observed at the beam interface. A typical 'X' cracks pattern was observed, since no joint hoops were provided at the joint. Spalling of concrete was observed during DR 4%.

In specimen J5, with shallow embedded length of about 50% of column depth, diagonal cracks did not occur; instead, a cone-shaped concrete breakout failure was observed. Spalling of concrete took place at DR 3%, at the portion where the breakout cone of top and bottom bars overlapped. The load decreased as a breakout cone formed and separated.

The shear strength of specimen J9 was very significant as initial cracks developed in the joint in the fifth to seventh cycle, but deformation occurred in the beam due to progressive increase of crack width at the beam interface and some more cracks in the length of beam. Remarkable crack controlling ability at the joint region was exhibited by specimen J9. No sign of side blowout was observed in any specimen, even where transverse reinforcement was not provided. Hence clear cover to the headed bar as $2d_b$ is sufficient to prevent side blowout.

Hysteretic performance

The load plotted against displacement graphs–hysteresis loops are shown in Figure 6. The load displacement hysteresis loop exhibited by specimen J1 is poor and verifies the weak performance of the joint. The joint exhibited very low strength owing to a lack of proper anchorage in the beam–column joint.

The results for J3 had shown that even the contribution of bond is negligible; head bearing provides sufficient anchorage, provided that the embedded length is equal to or more than $11d_b$.

Specimen J4, although it failed in the joint, exhibited a satisfactory hysteretic response up to DR 3%. This observation highlighted that a certain level of performance can be achieved with headed bars even without joint hoop reinforcement. The headed bar had the advantage of transfer of a more uniform distribution of compressive stress to the concrete at the headed end. This enables the development of a wider compressive strut in the joint, which enhances the joint shear strength. The hysteresis loops for specimens J2 and J9 are wide and stable, with higher energy dissipation in each primary loading cycle. In all the specimens it was

(a) (b) (c) (d) (e) (f)

Figure 5. Crack pattern of specimens: (a) J1; (b) J2; (c) J3; (d) J4; (e) J5; (f) J9

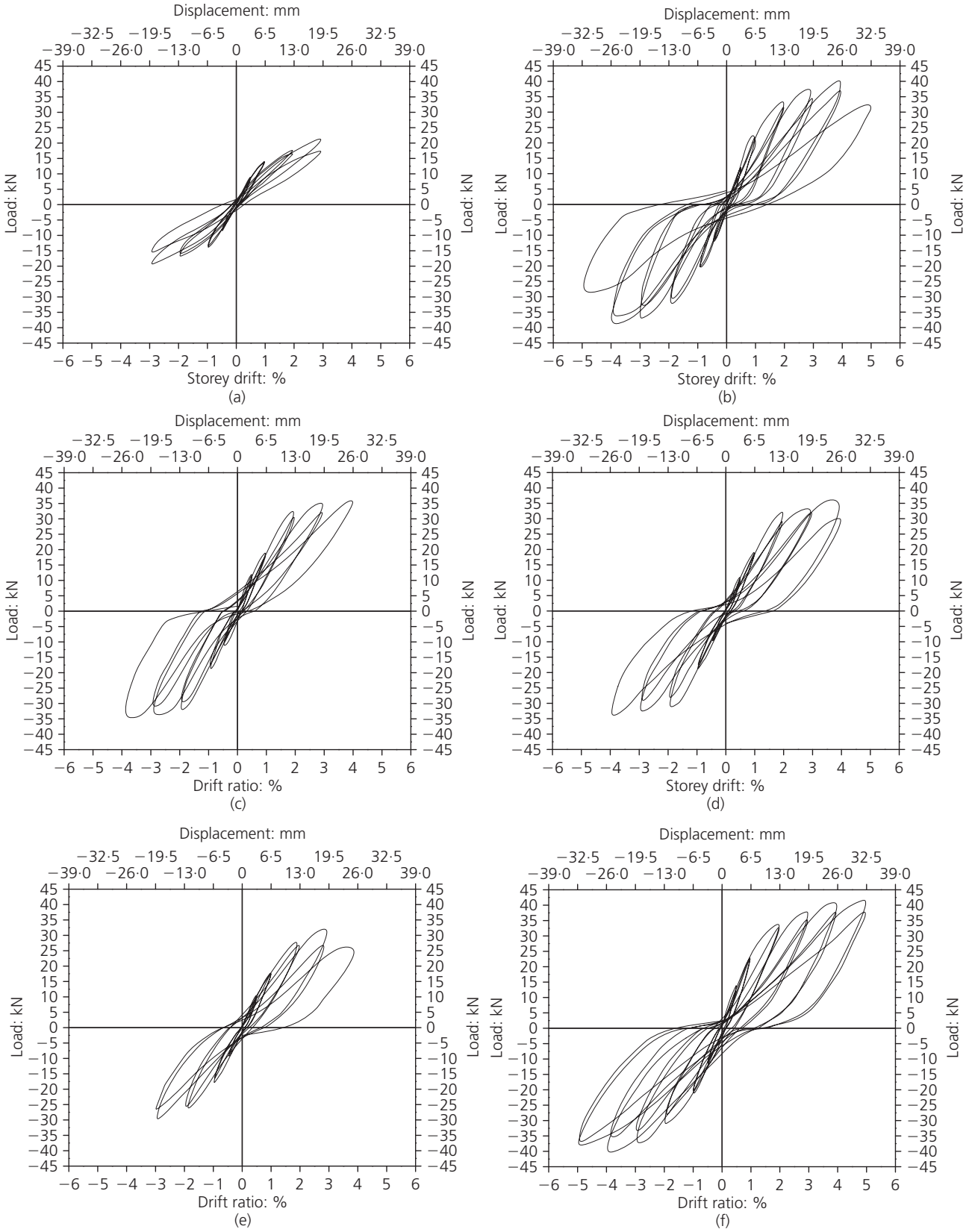

Figure 6. Load–displacement hysteresis loops of specimens: (a) J1; (b) J2; (c) J3; (d) J4; (e) J5; (f) J9

observed that the repeated loading cycle dissipated less energy than the primary loading cycle for each respective drift ratio.

Energy dissipation

The energy dissipated at the beam–column joint specimens through plastic deformation was the sum of the area in the beam tip load–displacement hysteresis loop. The cumulative dissipated energies for all specimens are given in Table 1 and Figure 7. The energy dissipated by specimens J3 and J4 is less than 50% that of J9. The energy dissipated by specimen J1 was very low owing to the joint shear failure that occurred at the lower displacement cycle. The best energy dissipation potential was exhibited by specimen J9 (20% more than J2), as the formation of a complete plastic hinge took place at the beam–column interface.

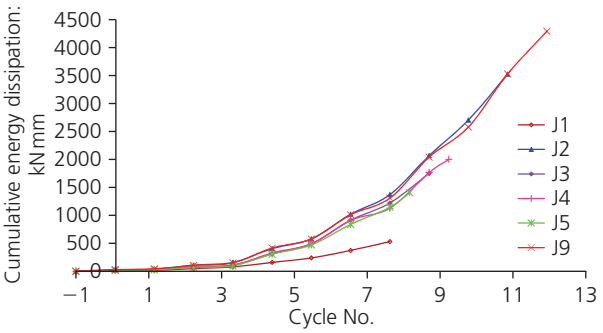

Figure 7. Cumulative energy dissipation

Displacement ductility

The displacement ductility (μ) is defined as Δ_{max}/Δ_y, where Δ_{max} is the vertical displacement at the loading point of the beam corresponding to P_{max}. The yield displacements, Δ_y, for all specimens were determined by extrapolation from measured vertical displacement at $0{\cdot}75P_n$ (Hwang *et al.*, 2005; Lee and Ko, 2007) in the 1% drift cycle except for specimen J1, where a 2% drift cycle was considered because of smaller peak load values at the initial drift cycles. The displacement ductility for all specimens is presented in Table 2. The specimen J1 exhibited lower displacement ductility because of short embedded length and no transverse shear reinforcement. For specimens J5, J4 and J3 displacement ductility is in the range 3·24–3·69. Displacement ductility of specimen J3 is somewhat higher than specimen J4. Specimen J9 exhibited large displacement ductility due to proper anchorage and the confining effect of transverse shear reinforcement.

Stiffness

Secant stiffness was used to provide a qualitative measure of the stiffness degradation in the specimens. In each cycle, secant

Specimen	Ultimate load, P_{max}: kN		Stiffness: kN/mm		Energy dissipation: kN mm	Mode of failure
	Upward direction	Downward direction	Initial	Final		
J1	21·63	19·80	2·75	0·86	530	JF
J2	40·70	39·20	3·96	0·95	3526	BJF
J3	36·12	34·59	3·69	1·36	1750	BJF
J4	36·90	35·20	3·42	1·39	2000	JF
J5	32·33	30·21	3·24	1·45	1407	Concrete breakout
J9	41·80	39·20	4·14	1·16	4293	BF

Table 1. Ultimate load, stiffness, energy dissipation and mode of failure of specimens

Specimen	Nominal flexural strength, M_n: kNm	Nominal flexural load, P_n: kN	Yield displacement, Δ_y: mm	Ultimate displacement, Δ_{max}: mm	Displacement ductility, Δ_{max}/Δ_y
J1	15·63	24·05	17·33	19·5	1·13
J2	15·63	24·05	5·60	26·0	4·64
J3	15·63	24·05	7·50	26·0	3·47
J4	15·63	24·05	7·73	26·0	3·36
J5	15·63	24·05	8·53	19·5	2·29
J9	15·63	24·05	6·00	32·5	5·42

Table 2. Nominal flexural strengths and displacement ductility of specimens

stiffness is the slope of a line drawn between maximum positive displacement points in the first half of the cycle to the maximum negative displacement point in the second half of the cycle. In Figure 8 the degradation of the secant stiffness is plotted against the corresponding number of cycles for each specimen tested. A similar trend of stiffness degradation with increased displacement cycle is observed for all specimens. Specimens J2 and J9 followed nearly the same path except for the 11th cycle, where specimen J2 exhibited more degradation of stiffness. Since many new cracks appeared and earlier cracks propagated further in the fifth cycle, rapid degradation of stiffness is observed in this cycle in both of the specimens.

Conclusion

An experimental study was performed to assess the anchorage strength of headed bars terminated within exterior beam–column joints with short development length. The tests were performed on six exterior beam–column joint specimens with and without transverse shear reinforcement. One specimen had 90° hook bars and the remaining specimens had headed bars. The test specimens were subjected to reverse cyclic loading. Based on the test results, the following conclusions were drawn.

(*a*) Clear cover to the headed bar as $2d_b$ is sufficient to prevent side blowout, even where transverse reinforcement is not provided.
(*b*) The beam–column specimen without transverse shear reinforcement can exhibit satisfactory seismic behaviour with headed bars up to a drift ratio of 3%; above this the role of transverse shear reinforcement is vital.
(*c*) The hysteretic behaviour of exterior beam–column joints with headed bars was superior to joints constructed with 90° bent bars with sufficient anchorage length.
(*d*) The combination of head size of circular shape $A_{brg}/A_b = 4$ with short development length $l_{dt} = 11d_b$ was sufficient to anchor the headed bar within the exterior beam–column joints, provided the headed end was placed within the diagonal compression strut.

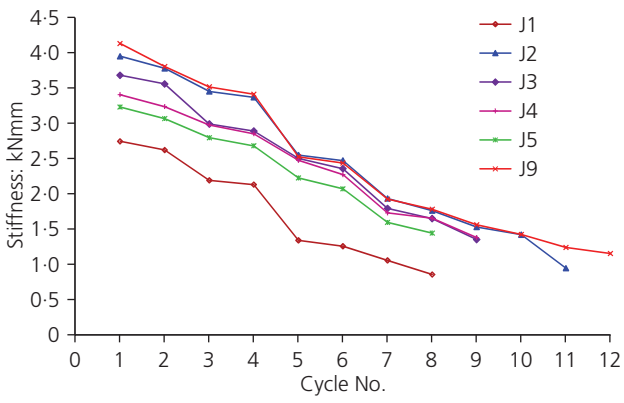

Figure 8. Stiffness degradation of test specimens

REFERENCES

ACI (American Concrete Institute) (2008) Committee 318: Building code requirements for structural concrete and commentary. ACI, Farmington Hills, MI, USA.

ACI–ASCE (2002) Committee 352R-02: Recommendations for design of beam–column connections in monolithic reinforced concrete structures. ACI, Farmington Hills, MI, USA.

Alva GMS, El Debs ALHDC and El Debs MK (2007) An experimental study on cyclic behavior of reinforced concrete connections. *Canadian Journal of Civil Engineering* **34(4)**: 565–575.

Bashandy TR (1996) *Application of Headed Bars in Concrete Members*. PhD thesis, University of Texas at Austin, Austin, TX, USA.

BIS (Bureau of Indian Standards) (1970) IS 383-1970 (reaffirmed 1997): Specification for coarse and fine aggregates from natural sources for concrete. Bureau of Indian Standards, New Delhi, India.

BIS (1991) IS 1489-1991: Portland pozzolana cement-specifications, Part 1 – Fly ash based. Bureau of Indian Standards, New Delhi, India.

BIS (1993) IS 13920-1993: Ductile detailing of reinforced concrete structures subjected to seismic forces. Bureau of Indian Standards, New Delhi, India.

BIS (2000) IS 456-2000: Plain and reinforced concrete – code of practice. Bureau of Indian Standards, New Delhi, India.

Chun SC, Lee SH, Kang THK, Oh B and Wallace JW (2007) Mechanical anchorage in exterior beam–column joints subjected to cyclic loading. *ACI Structural Journal* **104(1)**: 102–112.

Chun SC, Bohwan O and Naito CJ (2009) Anchorage strength and behaviour of headed bars in exterior beam-column joints. *ACI Structural Journal* **106(5)**: 579–590.

Hwang SJ, Lee HJ, Liao TF, Wang KC and Tsai HH (2005) Role of hoops on shear strength of reinforced concrete beam–column joints. *ACI Structural Journal* **102(3)**: 445–453.

Kang THK, Ha SS and Choi DU (2010) Bar pullout tests and seismic tests of small-headed bars in beam–column joints. *ACI Structural Journal* **107(1)**: 32–42.

Kotsovou G and Mouzakis H (2011) Seismic behaviour of RC external joints. *Magazine of Concrete Research* **63(4)**: 247–264.

Lee HJ and Ko JW (2007) Eccentric reinforced concrete beam–column connections subjected to cyclic loading in principal directions. *ACI Structural Journal* **104(4)**: 459–467.

Park R and Paulay T (1974) The art of detailing. In *Reinforced Concrete Structures*. Wiley, New York, USA, pp. 716–759.

Patel PA, Desai AK and Desai JA (2013) Evaluation of RC and SFRC exterior beam–column joint under cyclic loading for reduction in lateral reinforcement of the joint region. *Magazine of Concrete Research* **65(7)**: 405–414.

Thompson MK, Ziehi MJ, Jirsa JO and Breen JE (2005) CCT nodes anchored by headed bars – Part I: Behaviour of nodes. *ACI Structural Journal* **102(6)**: 808–815.

Wallace JW, McConnell SW, Gupta P and Cote PA (1998) Use of headed reinforcement in beam-column joints subjected to earthquake loads. *ACI Structural Journal* **95(5)**: 590–606.

Wright JL and McCabe SL (1997) *The Development Length and Anchorage Behaviour of Headed Reinforcing Bars*. The University of Kansas, Center for Research, Lawrence, Kansas, SM report No. 44, Structural Engineering and Engineering Materials.